Microplastics in human urine: Characterisation using µFTIR and sampling challenges using healthy donors and endometriosis participants

Jeanette M. Rotchell [a,b,*], Chloe Austin [a], Emma Chapman [a], Charlotte A. Atherall [c], Catriona R. Liddle [c], Timothy S. Dunstan [a], Ben Blackburn [a], Andrew Mead [d,e], Kate Filart [c], Ellie Beeby [c], Keith Cunningham [f], Jane Allen [e], Hannah Draper [c,f], Barbara-ann Guinn [c,**]

[a] School of Natural Sciences, University of Hull, Kingston-upon-Hull HU6 7RX, United Kingdom
[b] College of Health and Science, University of Lincoln, Brayford Pool, Lincoln LN6 7TS, United Kingdom
[c] Centre for Biomedicine, Hull York Medical School, University of Hull, Kingston-upon-Hull HU6 7RX, United Kingdom
[d] School of Life Sciences, University of Bedfordshire, Luton LU1 3JU, United Kingdom
[e] Department for Comparative Biomedical Sciences, The Royal Veterinary College, Hertfordshire AL9 7TA, United Kingdom
[f] Hull and East Yorkshire Endometriosis Centre, Castle Hill Hospital, Cottingham HU16 5JQ, United Kingdom

ARTICLE INFO

ABSTRACT

Microplastics (MPs) are found in all environments, within the human food chain, and have been recently detected in several human tissues. The objective herein was to undertake an analysis of MP contamination in human urine samples, from healthy individuals and participants with endometriosis, with respect to their presence, levels, and the characteristics of any particles identified. A total of 38 human urine samples and 15 procedural blanks were analysed. MPs were characterised using µFTIR spectroscopy (size limitation of 5 µm) and SEM-EDX. In total, 123 MP particles consisting of 22 MP polymer types were identified within 17/29 of the healthy donor (10 mL) urine samples, compared with 232 MP particles of differing 16 MP polymer types in 12/19 urine samples from participants with endometriosis. Healthy donors presented an unadjusted average of 2589 $\pm$ 2931 MP/L and participants with endometriosis presented 4724 $\pm$ 9710 MP/L. Polyethylene (PE)(27%), polystyrene (PS)(16%), resin and polypropylene (PP)(both 12%) polymer types were most abundant in healthy donor samples, compared with polytetrafluoroethylene (PTFE) (59%), and PE (16%) in samples from endometriosis participants. The MP levels within healthy and endometriosis participant samples were not significantly different. However, the predominant polymer types varied, and the MPs from the metal catheter-derived endometriosis participant samples and healthy donors were significantly smaller than those observed in the procedural blanks. The procedural blank samples comprised 62 MP particles of 10 MP polymer types, mainly PP (27%), PE (21%), and PS (15%) with a mean $\pm$ SD of 17 $\pm$ 18, highlighting the unavoidable contamination inherent in measurement of MPs from donors. This is the first evidence of MP contamination in human urine with polymer characterisation and accounting for procedural blanks. These results support the phenomenon of transport of MPs within humans, specifically to the bladder, and their characterisation of types, shapes and size ranges identified therein.

1. Introduction

Microplastics (MPs) are synthetic polymer particles in the micro size range and while an international agreement on size range has not been reached, the typical range is between 1 µm and 5 mm (Hartmann et al., 2019). MPs have been identified across all environments (GESAMP,

2015; Jenner et al., 2021, Jenner et al., 2022a) in food, drinking water (Danopoulos et al., 2020a, 2020b), and in human tissue samples including stool (Schwabl et al., 2019; Zhang et al., 2021), blood (Leslie et al., 2022), cadaver lung (Amato-Lourenco et al., 2021), lung (Jenner et al., 2022b), colon (Ibrahim et al., 2021), liver (Horvatits et al., 2022), placenta (Ragusa et al., 2021), breast milk (Ragusa et al., 2022), vein

---

(Rotchell et al., 2023) and testis/sperm (Zhao et al., 2023). A small-scale recent urine study, using six donors (aged 16–35 years old), detected four MP polymer fragments: polyethylene vinyl acetate (PVA), polyvinyl chloride (PVC), PP, and PE of 4–15 μm size range (Pironti et al., 2023).

MP exposure investigations using human cell and tissue approaches have revealed various impacts; with inflammatory and oxidative stress type responses reported (for review: Danopoulos et al., 2021). Other than cell and tissue culture studies, the clinical implications of MPs

Table 1
MP levels detected in endometriosis participant and healthy donor urine samples.

ID	Sex	Age	Sample collection date	State	MP/L †	MP/L ††	MP/L †††
Endometriosis participants, healthcare setting							
E1	F	28	04/2022	DE	0		-
E2	F	42	04/2022	DE	400		-
E3	F	41	04/2022	DE	1600		-
E4	F	38	05/2022	DE	1200		-
E5	F	36	05/2022	DE	1600		-
E6	F	30	05/2022	DE	36,000		PTFE, 32,160
E7	F	34	05/2022	DE	400		-
E8	F	37	06/2022	DE	0		-
E9	F	39	06/2022	DE	0		-
E10	F	26	06/2022	DE	4000		resins, 3520
							nylon, 800
E11	F	39	11/2022	DE	2527		nylon, 2000
E12	F	46	12/2022	DE	6600		-
E13	F	28	12/2022	DE	2544		-
Mean		**36**			**4375**	**4353**	**2960**
SD		**6**			**9689**	**9669**	**8865**
Endometriosis participants, using metal catheter							
E14A	F	41	06/2023	DE	28,000		PE, 6320
E14B	F	41	06/2023	DE	8800		PE, 23,520
E15	F	36	07/2023	DE	0		-
E16	F	31	08/2023	DE	0		-
E17	F	35	08/2023	SE	0		-
E18	F	38	08/2023	DE	800		-
E19	F	33	08/2023	DE	0		-
Mean		**36**			**5371**	**5365**	**4263**
SD		**4**			**10,489**	**10,483**	**8812**
All endometriosis participants combined							
Mean		**36**			**4724**	**4710**	**3416**
SD		**5**			**9710**	**9696**	**8635**
Healthy donors, own bathroom, no guidance given							
H1	F	39	06/2014	healthy	400		-
H2	F	54	06/2014	healthy	8000		EVA, 2400
H3	F	33	07/2014	healthy	1600		-
H4	F	50	06/2014	healthy	2800		-
H5	F	31	06/2014	healthy	3200		-
H6	F	50	06/2014	healthy[a]	9600		-
H7	F	44	05/2014	healthy[b]	0		-
H8	F	41	06/2014	healthy	1600		-
H9	F	23	05/2014	healthy	400		-
H10	F	32	05/2014	healthy	4000		-
H11	F	68	06/2014	healthy	800		-
H12	M	33	06/2014	healthy	800		-
H13	F	73	06/2014	healthy	1200		-
H14	F	79	062014	healthy	2800		PES, 2000
Mean		**46**			**2657**	**2635**	**338**
SD		**17**			**2874**	**2854**	**830**
Healthy donors, own bathroom and guidance given							
H15	F	26	07/2023	healthy	8400		PP:PE, 2000
							PTFE, 3200
H16	F	26	07/2023	healthy	2000		-
H17	F	31	07/2023	healthy	800		-
H18	F	30	07/2023	healthy	800		-
H19	F	38	07/2023	healthy	0		-
Mean		**30**			**2400**	**2394**	**1040**
SD		**5**			**3429**	**3423**	**2326**
All heathy donors combined							
Mean		**42**			**2589**	**2575**	**533**
SD		**16**			**2931**	**2917**	**1365**

Abbreviations: † unadjusted, †† blank subtracted, ††† LOD/LOQ adjusted values. DE = deep endometriosis, SE = superficial endometriosis. [a]Level 3 dyskaryosis, [b]benign schwannoma. – Did not meet LOQ criteria. AC, acrylic; EVA/EVOH, ethylene-vinyl acetate/ethylene vinyl alcohol; PBA, polybutylacrylate; PDMS, polydimethyl siloxane; PP, polypropylene; PP/PE, polypropylene polyethylene co-polymer; PTFE, polytetrafluoroethylene; PS, polystyrene; PE, polyethylene; PES, polyester; PUR, polyether urethane; SP, silicone polymer; PET, polyethylene terephthalate; SP, silicone polymer.

within the human body have yet to be determined. Evidence is emerging however, that high MP levels are associated with inflammatory disorders, specifically bowel disease (Yan et al., 2021).

Endometriosis is a common, chronic, and most relevantly here, inflammatory, gynaecological disease characterised by the presence of endometrial-like tissues outside of the uterine cavity. Endometriotic deposits are most found in the ovaries, fallopian tubes and pelvic cavity but are also described in distant locations such as the pleural cavity and surgical scars. Despite being thought to affect up to 1 in 10 women, the pathogenesis of endometriosis remains poorly understood. Retrograde menstruation, or the efflux of shed endometrial fragments and blood into the pelvic cavity via the fallopian tubes plays a major role in the initiation of endometriosis. Although this fluid is rich in proteins, immune cells and endometrial stem-cells, this mechanism is not sufficient to explain the initiation of endometriosis since retrograde menstruation is almost universal. Other theories have been proposed including retrograde menstruation, coelomic metaplasia, immunological factors, endometrial stem cells and lymphatic or hematogenous spread (Signorile et al., 2022). It is likely that the aetiology is multifactorial with genetic, environmental, hormonal, and immunological factors (Abramiuk et al., 2022).

This study aims to identify any MP particles present in digested human urine samples, while also accounting for procedural blank contamination. Urine samples have been provided by healthy individuals and participants affected by endometriosis for direct comparison. Particles isolated from urine have been chemically characterised using μFTIR spectroscopy (with a 5 μm lower size limit of detection) along with a subset characterised using SEM-EDX to provide additional validation.

2. Methods

2.1. Human tissue acquisition

Urine samples were collected from participants attending the Hull and East Yorkshire Endometriosis Centre at Castle Hill Hospital, Hull University Teaching Hospitals NHS Trust and from healthy donors (from within their own home environment within the U.K.; Table 1). Participants attended for elective laparoscopy to diagnose or treat deep endometriosis (DE) and gave informed consent to take part in this NHS Research Ethics Committee and Health Research Authority approved study (REC reference 19/WA/0121). Deep endometriosis is defined here as the disease invading at least 5 mm below the tissue surface confirmed by laparoscopy. The first batch of samples of urine were collected from healthy donors and endometriosis participants (Table 1) between the dates May - June 2014 and April - June 2022 respectively. The healthy donor urine samples collected between May and June 2014, had ethical approval from the Faculty of Creative Arts, Technologies and Sciences ethics committee at the University of Bedfordshire (15 May 2013, Ethics ref: H072). Ethical approval for the analysis of these urine samples at the University of Hull were provided by the Faculty of Science and Engineering Ethics Committee in 2017 (Ethics Ref: FEC_41_2017) and by the Hull York Medical School Ethics Committee in 2022 (REC Ref: 21–22 65).

A second batch of urine samples were collected from healthy donors within their own homes and participants with endometriosis, under anaesthesia, using a metal catheter (Table 1) between the dates June – August 2023. Mid-stream urine samples were collected using sterile universal containers pre-operatively, and assessed for contamination using urinalysis (Siemens Multistix GP Reagent Strips). Urine samples were aliquotted and stored frozen. Digestion of n=38 samples (batch 1: 14 healthy, 13 endometriosis; batch 2: 5 healthy, 6 endometriosis) in total were conducted with at least one procedural blank per batch. From the point that a donor produces their sample, there is unavoidable scope for the sample to be open to the indoor air environment. Urine samples from healthy donors were produced within the volunteer's own home

environment. Those from the endometriosis participants were produced within a medical setting. The participant sample size was based on our previous analysis of mussel and human tissue samples (Li et al., 2018; Jenner et al., 2022b).

The procedural blanks consisted of two batches, batch 1 was n=7 blanks from the medical setting, involving endometriosis participants or healthcare professionals mimicking the production of a sample, opening, closing a vial for a similar time span. A further n=3 blanks were added to batch 1, using pre-filtered water as proxy for a urine sample decanted into the sampling vial by a healthcare professional within the medical setting. For batch 2 of the procedural blanks, a further n=5 procedural blanks were initiated in healthy donor home environments after the provision of guidance to entirely mimic the process of removing clothing, sitting, pouring the pre-filtered dH_2O into Colli-Pee® tubes in close vicinity of the body (to theoretically sample any close body-associated textile-type particles). The volume analysed was ~10 mL of freshly defrosted urine. Endometriosis participants mean age was 36 ± 5 years (range 26–46), while healthy donor mean age was 42 ± 16 years (range 23–79), all samples were from female participants and healthy volunteers except sample H12 (Table 1).

2.2. Urine sample digestion and filtration

Urine samples (n=38) were placed in hydrogen peroxide (100 mL of 30% H_2O_2) alongside procedural blanks (n=15). Flasks were placed in a shaking incubator at 60 °C for approximately 7 days, 80 rpm. The digest, adapted from previous studies investigating MPs within different environmental and tissue samples (Jenner et al., 2022b), promotes removal of organic particles while maintaining MP integrity (Munno et al., 2018). Samples were then filtered onto aluminium oxide filters (0.02 μm Anodisc, Watford, U.K.) using a glass vacuum filtration system. These were stored in petri dishes before chemical composition analysis alongside blanks.

2.3. Chemical characterisation of particles using μFTIR analysis

Each tissue sample Anodisc filter was placed onto the μFTIR spectroscopy platform, and the length (largest side) and width (second largest side) recorded using the aperture height, width, and angle size selection tool, available with the ThermoScientific Omnic Picta Nicolet iN10 microscopy software. Particles were given a shape category (fibre, film, fragment, foam, or sphere (Free et al., 2014)), with fibrous particles characterised as having a length to width ratio > 3 (Vianello et al., 2019). Where the particle shape was ambiguous the term 'irregular' was noted instead and could represent either fragment or film. μFTIR analysis was conducted in liquid nitrogen cooled transmission mode (Nicolet iN10, ThermoFisher, Waltham MA, U.S.A.). The cooled mercury cadmium telluride (MCT) detector facilitated the analysis of particles *accurately* down to ~5–10 μm in size. The Nicolet iN10 microscope used has a 15 × 0.7 N.A. high efficiency objective and condenser, as well as a colour CCD digital video camera with an independent reflection and transmission illuminations mounted, for capturing images of particles. This model has standardised 123× magnification with the aperture settings used. A quarter of each filter, containing the total digested urine sample, was analysed. A background reference spectrum was first recorded. μFTIR parameters were; spectral range of 4000–1250 cm^{-1}, high spectral resolution 8 cm^{-1}, scan number of 64. Smoothing, baseline correction and data transformation were not used. Resulting sample spectra were compared to a combination of polymer libraries (Omnic Picta, Omnic Polymer Libraries) and full spectral ranges were used with a match threshold of $\geq 70\%$. If particles were below the $\geq 70\%$ match index threshold, three attempts were made to collect a successful match before moving on to the next particle undergoing analysis. Particles below $\geq 70\%$ match, and particles not classified as a plastic were recorded but not included in the results shown (Cowger et al., 2020). The total number of particles (MPs and others) identified was 2868, for

which 295 (10.3%) were MPs. Only the MPs data are presented in the results.

2.3.1. SEM/EDX analyses

SEM/EDX analysis was conducted on a targeted subset (n=3) of individual candidate MPs selected by µFTIR using the anodisc filters described above for validation purposes. SEM/EDX screening used surface morphology and elemental composition to determine whether each particle was potentially of plastic polymer composition. The analysis was conducted using a Zeiss EVO 60 instrument and Oxford Instruments X-Max 80 detector. The SEM was run in the charge reducing variable pressure mode (chamber pressure of 10 Pa) which allows the imaging of electrically non-conductive samples without the application of a conductive coating. The SEM provided low resolution imaging of particle surface structures (not shown), as well as elemental composition signatures. Spectra of the chemical composition of the debris analysed were then compared with those already present in literature. The integration between results obtained by SEM and EDX methods and taking into consideration that samples were previously digested with hydrogen peroxide solution which means that many organic compounds were excluded from the dataset, and allows establishing whether the analysed samples were plastics or not, adding weight to the µFTIR dataset.

2.4. Quality assurance and control measures

Strict control measures were used to quantify and characterise the nature of any unavoidable background contamination. Due to the ubiquitous nature of MPs in the air, contamination of urine samples is likely during collection. While it was not possible to control this, each sample was placed immediately in a glass vial. In parallel, procedural blanks (n=15, comprised of two batches consisting of n=10 and n=5) were initiated at the time and point of urine collection from the endometriosis participant donors within the same participant toilet and decanted in the same hospital sluice area. The procedural blank mimicked the entire sample processing steps but lacked the urine sample. Seven procedural blanks contained air from the clinical room/open to the air only, three used pre-filtered distilled water as a surrogate for urine. A second batch of n=5 procedural blanks were conducted by healthy donors from their home environments using pre-filtered distilled water decanted into a tube near their body while unclothed.

All reagents were pre-filtered and prepared in bulk. MPs found within procedural blanks represent contamination from indoor atmosphere at the point of urine collection, contamination from laboratory reagents, equipment or fallout from the air during the transfer of samples. No standardised protocols are currently adopted within the MPs research field to account for background contamination, so multiple contamination adjustments were applied in this study for comparison (Table 1). Two approaches were used: subtraction, which is routinely used in the MP research field, and a limit of detection (LOD) and limit of quantification (LOQ) approach (Horton et al., 2021). Presenting raw data, subtraction, and LOD/LOQ adjusted results allows a comparison for each technique (Table 1).

The H_2O_2 used was triple filtered using an all-glass vacuum filtration kit and 47 mm glass fibre grade 6 filters (GE Healthcare Life Sciences, Marlborough MA, U.S.A.). All glassware underwent thorough manual cleaning, before a dishwasher cycle using distilled water and then a manual three rinse wash with triple filtered MilliQ water. All equipment and reagents were always covered with foil lids and a small opening made when pouring. Additionally, when filtering digested samples, glassware and the sides of the filtration kit were rinsed three times with triple filtered MilliQ water to avoid sample particle loss. Each tissue sample was processed individually to prevent cross contamination. Plastic equipment was avoided, a cotton laboratory coat, and a new set of nitrile gloves for each sample processing step were used.

2.5. Statistical analysis

Tests for homogeneity and significance were performed on unadjusted MP values using SPSS. All data were determined not normally distributed with a Shapiro-Wilk test and a Kruskal-Wallis test applied. There are no standardised methods for the calculation of MP concentrations available at present, herein three are presented: unadjusted, mean of the procedural blank values, regardless of polymer type, subtracted, and an LOD/LOQ method (Horton et al., 2021).

3. Results

3.1. MP abundance levels detected in human urine samples

In total, 355 MP particles (from one quarter of each filter analysed) were characterised from all the 10 mL healthy and endometriosis urine samples combined. These consisted of 22 MP polymer types in total identified, 18 types from 17 out of the 19 healthy donor 10 mL urine samples, with an unadjusted average of 2589 $\pm$ 2931 MP/L (range 0–9600 MPs) (Fig. 1, Table 1). Urine from the endometriosis participants contained 16 MP polymer types in 12 out of 19 urine samples and a mean of 4724 $\pm$ 9710 MP/L of urine (0–36,000) (Fig. 1, Table 1), which did not significantly differ from the healthy donor values (p=0.38). The MP levels in neither the healthy donor nor endometriosis urine samples differed significantly from the procedural blank samples (p=0.355 and 0.826). The combined blanks contained 17 $\pm$ 18 MPs per sample (range 0–68 MPs) with 13 MP types that differed in terms of the dominant polymer types detected compared with the urine samples.

After subtracting background contamination, regardless of polymer type, this value becomes 2575 $\pm$ 2914 MP/L for all healthy samples combined, and 4710 $\pm$ 9696 MP/L for endometriosis urine samples combined (Table 1). Using only those MPs that meet the LOD/LOQ criteria, the mean value reduces to 533 $\pm$ 1365 MP/L for healthy samples and 3416 $\pm$ 8635 MP/L for endometriosis urine samples. The MP polymers PE (E14A, E14B), PP:PE (H15), PTFE (H15, E6), resins (E10), nylon (E10, E11), ethylene vinyl acetate (EVA) (H2), and PES (H14) were above the LOD and LOQ for urine samples from each donor where indicated (S1 Table).

3.2. MP particle characterisation from urine samples

Of the MPs detected in urine samples, PE (27%), PS (16%), resins (12%), and PP (12%) polymer types were most abundant in healthy donor samples (Fig. 2A, Fig. 3), compared with PTFE (59%), and PE (16%) in samples from endometriosis participants (Fig. 2B, Fig. 3). MP particles identified within the healthy donor urine samples had a mean particle length of 61.92 $\pm$ 51.15 µm (range 19–400 µm), and a mean particle width of 34.85 $\pm$ 19.63 µm (range 10–128 µm)(Fig. 4), where the length and width were significantly smaller in size (p=<0.001 for both dimensions) compared with the procedural blank particles. MPs shapes from healthy urine donors were predominantly fragments (66%) and film (30%) of clear/white colour (89%)(Fig. 5A). MP particles identified within all endometriosis participant urine samples combined had a significantly larger mean particle length (p=0.007 compared with procedural blanks) of 119.01 $\pm$ 113.28 µm (range 15 – >300 µm), and a significantly larger mean particle width of 79.09 $\pm$ 87.73 µm (range 9 – >300 µm) relative to the healthy donor samples (p=<0.001) (Fig. 4). Separating the catheter derived urine samples from the endometriosis participant-provided samples (within a healthcare toilet setting) resulted in a significant difference in the size ranges observed as follows. Metal catheter-derived MPs only were of length, 31.98 $\pm$ 21.97 µm and width, 21.88 $\pm$ 11.80 µm, which compares with participant-provided at healthcare-setting toilet: length, 177.45 $\pm$ 112.36 µm and width 117.49 $\pm$ 95.44 µm, significantly smaller (p=<0.001) for both size dimensions. MPs shapes from endometriosis participant urine were predominantly fragments (95%) plus small numbers of film (4%) and fibres (<1%) and
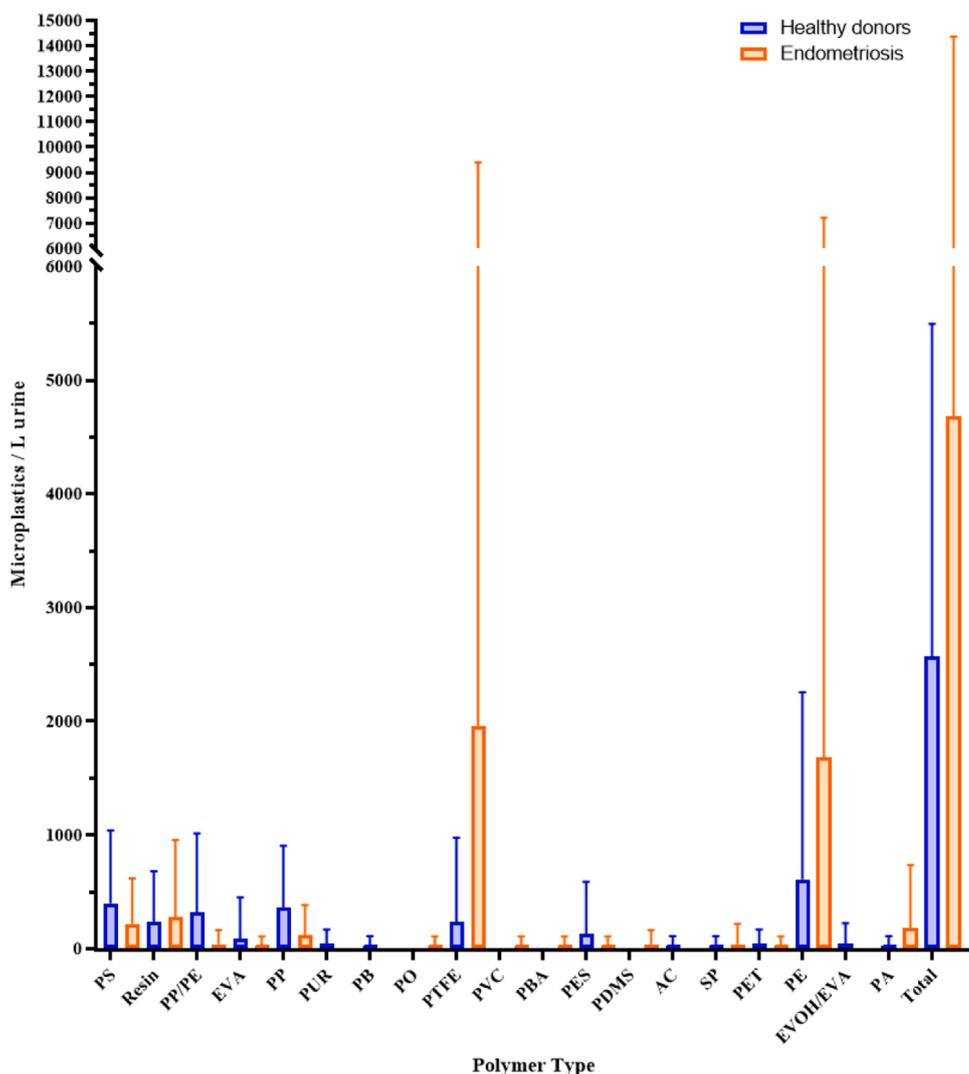
Fig. 1. Total number of MPs in healthy and endometriosis urine samples. Abbreviations: AC, acrylic; EVA/EVOH, ethylene-vinyl acetate/ethylene vinyl alcohol; PB, polybutadiene; PBA, polybutylacrylate; PDMS, poly-dimethyl siloxane; PP, polypropylene; PP/PE, polypropylene polyethylene co-polymer; PTFE, Polytetrafluoro-ethylene; PA, polyamide (nylon); PO, polyolefin; PS, polystyrene; PE, polyethylene; PES, polyester; PUR, polyether urethane; resins, epoxy- hydrocarbon- phenoxy-resins; SP, silicone polymer; PET, polyethylene terephthalate; PVC, polyvinyl chloride; SP, silicone polymer.

of clear/white colour (96%)(Fig. 5B).

3.3. SEM/EDX analysis

SEM/EDX analyses provided high resolution pictures of the particles surface structure of the fragments analysed, as well as their elemental composition signatures. This information was used to verify a small subset of MP compositions obtained using the µFTIR approach. According to the literature, PP and PE show a strong Carbon EDX peak (Wang et al., 2017), which have been observed (Fig. 6). Examples of spectra from an epoxy resin fragment, identified as such by µFTIR, is also shown (Fig. 6) where it is easy to see the Carbon peak (C) and other few additional elements characteristic of other plastic types.

3.4. Non-MP chemical characterisation

Several non-MP, yet related, as either MP building block polymer monomers or polymer additives, were also observed as follows: the most prevalent chemical detected was N-(2-ethoxyphenyl)-N-(2-ethyl-phenyl)-ethanediamide which were detected in 63% (12/19) healthy donors and 47% (9/19) from endometriosis participants. Bisphenol A propoxylate/ethoxylate (within three healthy donor urine samples), bis

(2-hydroxyethyl) dimerate (healthy donor sample), and tetraammonium octamolybdate (in an endometriosis participant urine sample) were plastic additives identified. Many particles (n=21) containing the insecticide 2,3-dichloro-1,4-naphtho-quinone were detected in urine from one participant with endometriosis. The most detected non-MP particle was cellulose fragments identified in 34 of the 38 human urine samples analysed, followed by zein fragments.

The MP levels within the procedural blank samples were not significantly different than those identified within procedural blanks but were comprised of different plastic polymer types. All blanks combined comprised n=62 MP particles of 10 MP polymer types, mainly PP (27%), PE (21%), and PS (15%) (Fig. 2C), with a combined mean ± SD of 17 ± 18 MP particles. These had significantly different mean particle length of 133.10 ± 94.32 µm (range 22 – >300 µm), and width of 59.92 ± 55.30 µm (range 7 – >300 µm) compared with the MP particles observed in the healthy donor ($p=<0.001$ for both dimensions) and all endometriosis participant urine samples combined ($p=0.007$ for length only for the latter samples). The catheter-derived endometriosis MPs were however significantly smaller than the blank MP particles ($p=<0.001$ in both dimensions). Blank MPs were predominantly fragment (84%) or fibre (10%) or film (5%)(Fig. 5C) of clear/white colour (95%). The MPs identified within the air-derived blanks (n=7) contained different types
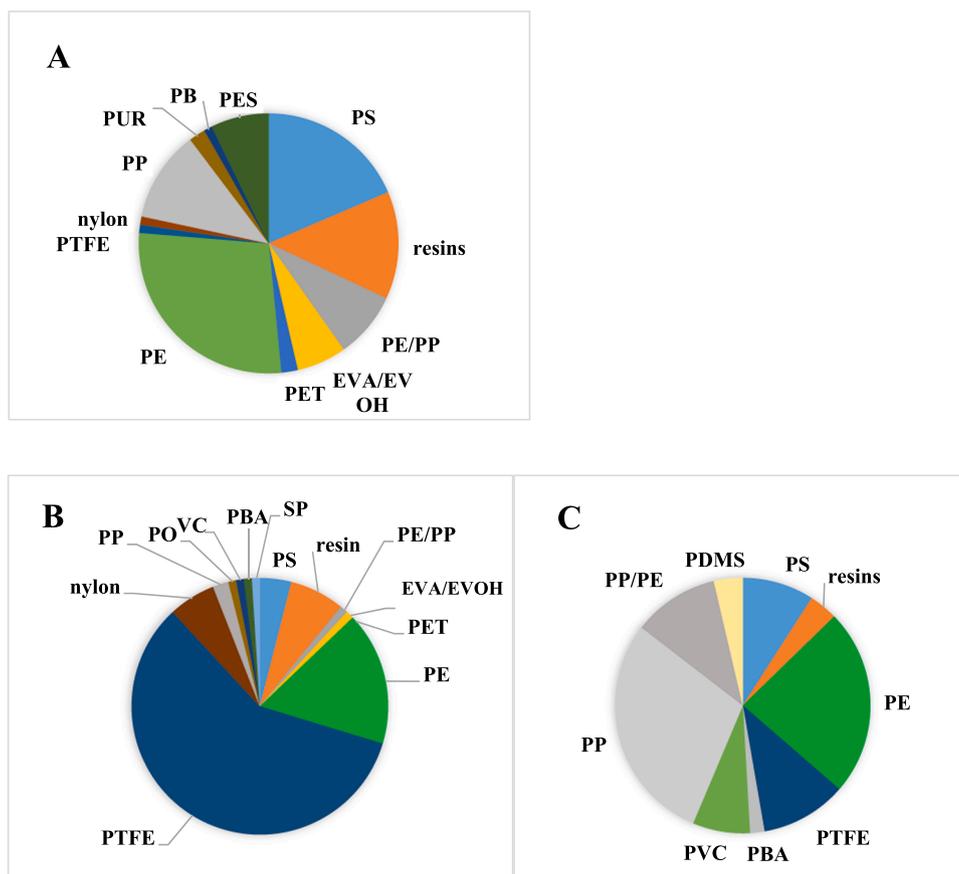
Fig. 2. Microplastic polymer types identified in A. healthy, B. endometriosis and C. procedural blank samples. Abbreviations: AC, acrylic; EVA/EVOH, ethylene-vinyl acetate/ethylene vinyl alcohol; PB, polybutadiene; PBA, polybutylacrylate; PDMS, poly-dimethyl siloxane; PP, polypropylene; PP/PE, polypropylene polyethylene co-polymer; PTFE, Polytetrafluoroethylene; PA, polyamide (nylon); PS, polystyrene; PE, polyethylene; PES, polyester; PO, polyolefin; PUR, polyether urethane; SP, silicone polymer; PET, polyethylene terephthalate; PVC, polyvinyl chloride.

(though not levels $p=0.247$) of 33 ± 27 MP particles and polymer types (PE>PTFE>PS/PVC) relative to those from the water-derived blanks (n=3) which contained 17 ± 14 MP particles and polymer types (PP>PE:PP copolymer) (Supplemental Material Fig S1).

4. Discussion

In this study, MPs have been isolated from urine samples from both healthy donors and endometriosis participants, with no significant difference in the levels detected between these two groups. The inter-individual variation in the levels of MPs in both groups was high, ranging from no MPs detected at all from four individuals to 36,000 MPs/L of urine for another individual. This individual variation was also observed in a pilot analysis conducted in Italy, whereby 2 of 6 individuals urine samples contained no MPs relative to four other donors (Pironti et al., 2023). In contrast however, the Italian donor study detected a maximum of n=3 MP particles per individual with no urine volume noted (Pironti et al., 2023)(Table S2). Assuming a typical void sample size of ~200 mL was analysed; this would equate to a maximum of ~15 MP/L urine which is significantly less than that detected in this study.

Of the MPs polymers detected in urine samples, PE (27%), PS (16%), and PP (12%) were most abundant in healthy donor samples (Fig. 2A, Fig. 3), compared with PTFE (59%) and PE (16%) in samples from participants with endometriosis (Fig. 2B, Fig. 3). Analysis of a small subset of the same particles characterised using µFTIR were also characterised using (a more labour intensive) SEM-EDX approach with similar results (Fig. 6). Categorical identification of each particle using either technique, either µFTIR or SEM-EDX, has limitations. µFTIR relies

on match to library spectra which are prepared using 'virgin' polymers, and particles that have been in the environment/an organism for any length of time may result in a spectrum that is somewhat different in terms of the main peaks. This weathering factor is addressed by selecting a library match threshold of 70%, as used in this study, and in general throughout the MP literature. The SEM-EDX images are interesting in that the 'smooth' appearance of the fragments, especially the epoxy resin particle (Fig. 6), add additional weight that these are anthropogenic source rather than natural polymers.

The urine samples from the healthy donors contained similar polymer types as those identified in the healthy donors in the Italian pilot study: PP and PE (Pironti et al., 2023). The endometriosis participant samples contained a high levels of PTFE fragments, though only in three individuals, and one healthy donor individual. PTFE fragments (and film/fibres) have previously been identified in 4 out of 11 participant lung tissue samples (Jenner et al., 2022b), yet PTFE was not found in another lung study by Amato-Lourenço et al., (2021) nor was it identified within the MPs detected in human blood (Leslie et al., 2022) or semen samples (Zhao et al., 2023). PTFE is used in a range of applications and is also referred to as its brand name Teflon. Originally discovered in the 1930 s and manufactured since the 1950 s, it is used as a non-stick coating and lubricant in products such as cookware, car interiors and dental floss, with limited reports in terms of human toxicology as a particulate (Pagedar et al., 2009; Choi et al., 2014). Teflon has been used in surgery applications leading to the condition of 'Teflon granuloma', which is an inflammatory giant-cell foreign body reaction to the PTFE fibre exposure (Pagedar et al., 2009). Another study reports small airway-centered granulomatous lesions in factory workers (n=3) at facilities that apply coatings to pans and other utensils, exposing them
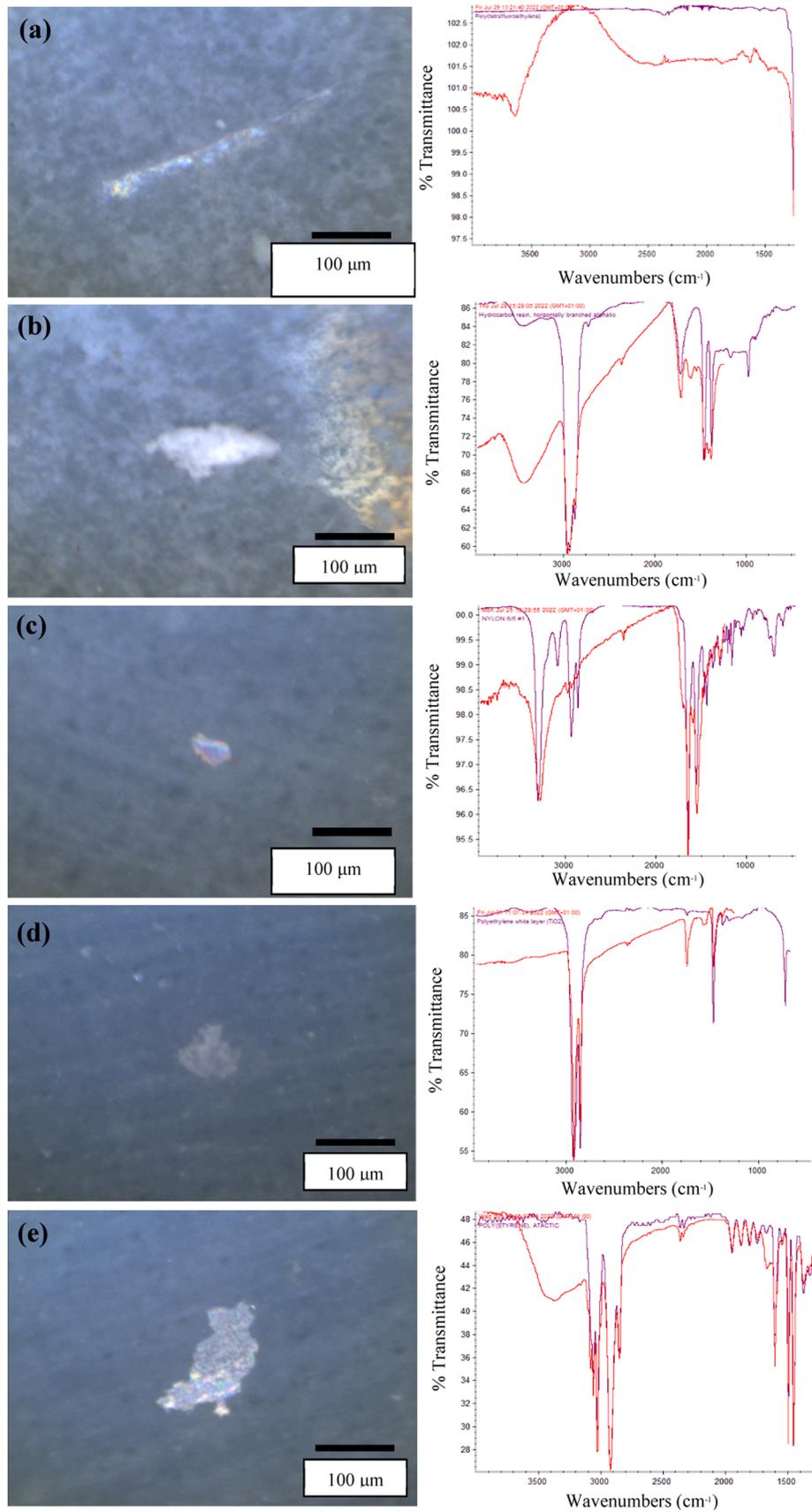
Fig. 3. Selected images of the MPs identified within urine samples alongside the spectra obtained: (a) PTFE fragment[E], (b) resin fragment[E], (c) nylon fragment[E], (d) PE fragment[H], (e) PS fragment[H]. [E], endometriosis participant. [H], healthy donor. Scale bar 100 µm. Abbreviations: PTFE, polytetrafluoroethylene; PE, polyethylene; PS, polystyrene.
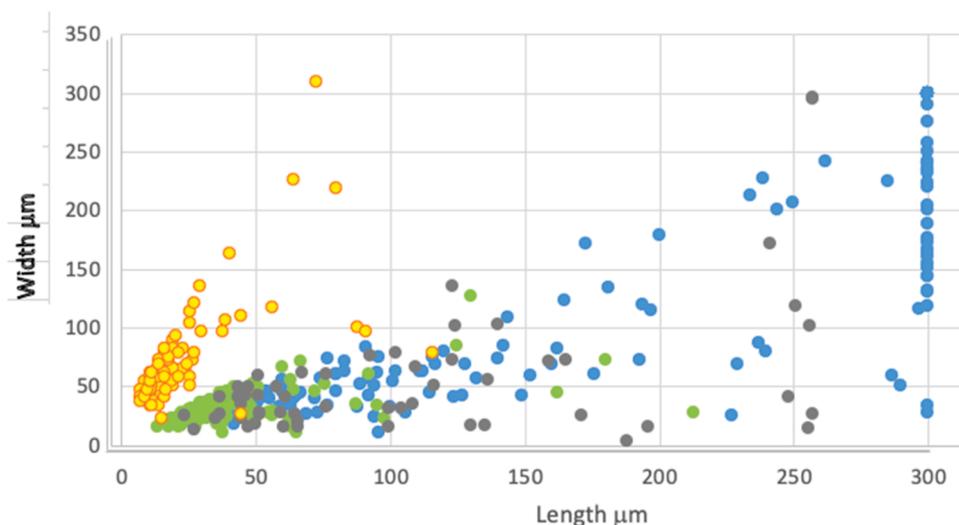
Fig. 4. Microplastic size dimension distributions. Healthy (green), participant-provided endometriosis (blue), catheter-provided endometriosis (yellow), and procedural blank (grey) samples.
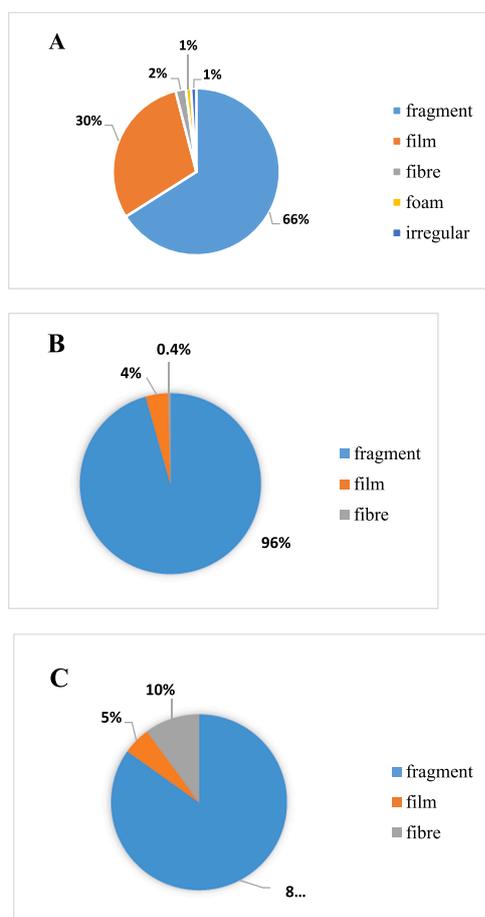
Fig. 5. Distribution of microplastic particle shapes: A. healthy donor urine, B. endometriosis participant urine, and C. procedural blank samples.

to constant PTFE particles (Choi et al., 2014).

The former are examples of physical particulate-related toxicity endpoints, yet PTFE is a fluoropolymer and an example of a 'forever chemical' belonging to the PFAS group of chemical contaminants. Their mechanisms of chemical toxicity in humans are numerous including immune suppression, thyroid function, liver disease, lipid dysregulation,

and endocrine disruption endpoints (for review: Fenton et al., 2021), and as such are currently subject to changing legislation and regulation, especially in their use for food packaging materials (Ramírez Carnero et al., 2021;). A mean level of ~230 and ~2000 PTFE-containing MPs/L within the healthy and endometriosis urine samples respectively represents a pool of potential leachates of the PFAS-type chemical if retained within the body. However, while exposure to high levels of PFAS (corresponding to a sum of all PFAS chemicals more than 10 µg/L) in drinking water has been associated with an increased risk of polycystic ovary syndrome and possibly uterine leiomyoma and infertility, no such association has been found for endometriosis (Hammarstand et al., 2021).

The physical characteristics of the MPs detected in the two donor groups varied with respect to size and shape, representing one way to differentiate the two groups. MP particles identified within the endometriosis catheter participant urine samples had a significantly smaller mean particle width relative to the healthy donor samples ($p=<0.001$). Endometriosis participant urine contained MP shapes that were split between fragments and films, while the healthy donor urine consisted of mainly fragments. The Italian study urine samples also consisted of mainly fragments, with no mention of film shapes (Pironti et al., 2023). MP shape has been identified as an important factor in terms of toxicity in cell-based exposure experiments whereby irregular shapes are correlated with inflammation and oxidative stress type impacts (Danopoulos et al., 2021). The size ranges observed in the urine samples are larger than the previous pilot urine analysis (range 7–15 µm, Pironti et al., 2023) but of a similar size range to those detected in human testis and sperm samples, which ranged from 21.76 µm to 286.71 µm (Zhao et al., 2023) as well as identified within human cardiac samples, which ranged from 20 µm to 469 µm (Yang et al., 2023). Human venous blood samples analysed in the same investigation also presented MPs ranging from 20 µm to 84 µm (Yang et al., 2023).

The size and shape characteristics of the MPs detected raise questions with respect to the fate and transport of such contaminants within the human body. Each human kidney weighs approximately 115–155 g in females, while male organs are slightly larger (by 10–20 g)(Molina and DiMaio, 2015). Nephrons carry out cleaning of the blood by particle size, consisting of a tubule (the Bowman's capsule) that surrounds capillaries of approximately 200 µm in diameter, comprising the glomerulus. These glomerular capillaries are the site of the blood filtration based on particle size. Particles take a route passing through the renal corpuscle, into a capillary arteriole, a capillary network, the peritubular capillaries, and vasa recta, before returning to the venous system. The mean length
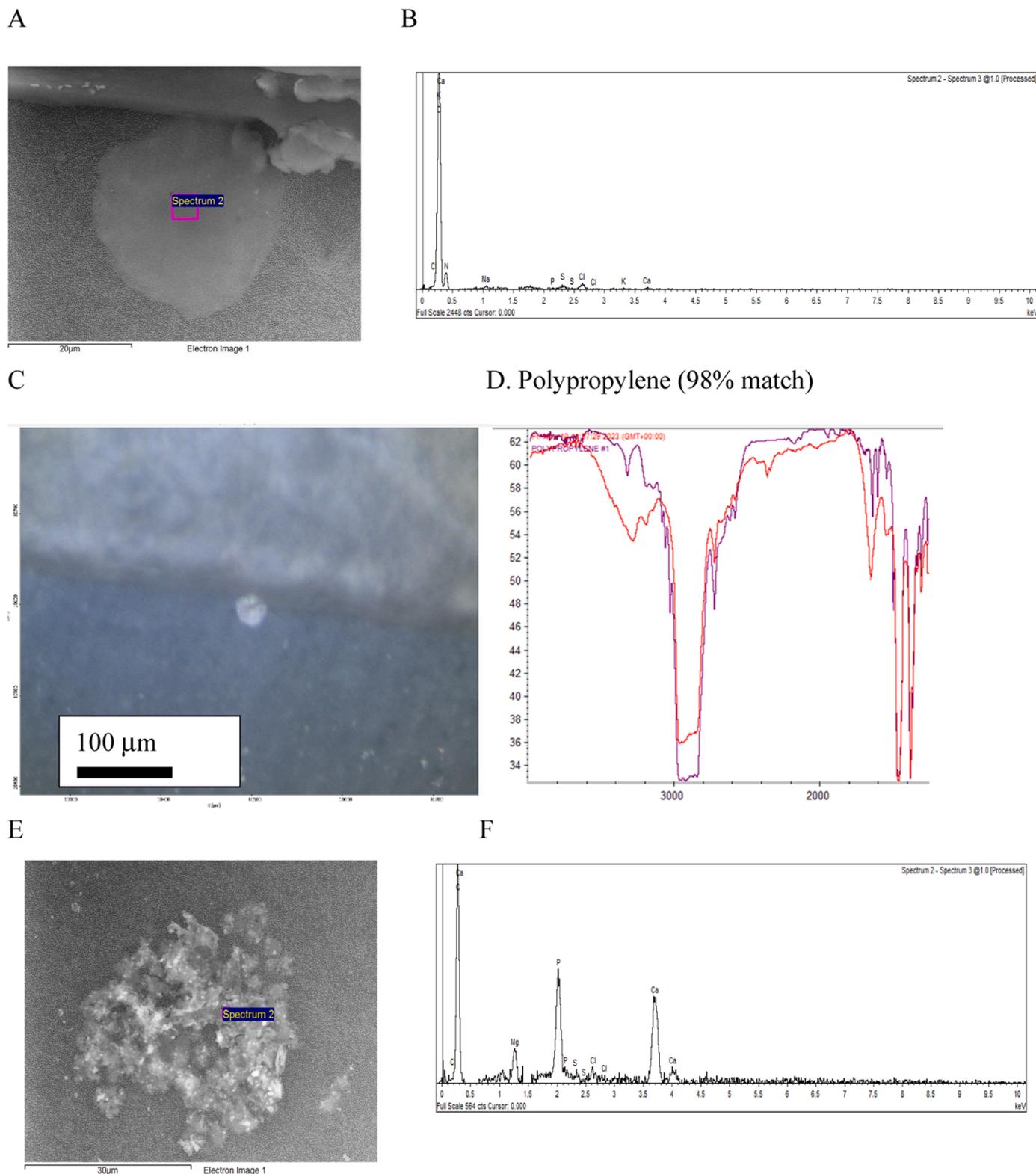
A

B

C

D. Polypropylene (98% match)

E

F

Fig. 6. SEM/EDX images and microanalysis from plastics identified via μFTIR as PP, PE and epoxy resin: SEM images (a, e, i) and spectra (b, f, j) showing the different kind of MP fragments obtained alongside the μFTIR obtained images (c, g, k) and spectra (d, h, l).

(representing the longest dimension) of all MPs for each donor type was ~62 μm (healthy) and ~119 μm (endometriosis) which, in theory, is too large to navigate the small capillary networks of the kidney to reach the bladder (Fig. 7).

Contrary to the current accepted paradigm of the endothelial-

capsular membrane acting as a barrier to all but small molecules (of 30–50 kDa size), there are reports of particles (up to 0.4 μm) and carbon nanotubes (0.2 – 0.33 μm) excreted with high aspect ratios (100:1–500:1) being cleared by glomerular filtration in mice (Ruggiero et al., 2010; Adhipandito et al., 2021). While such published dimensions
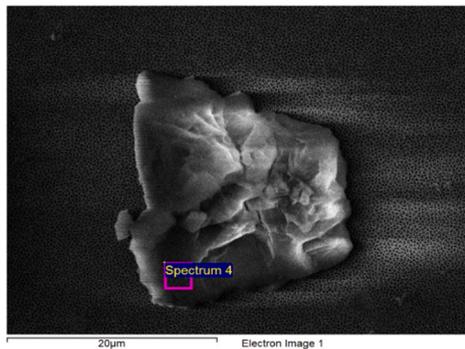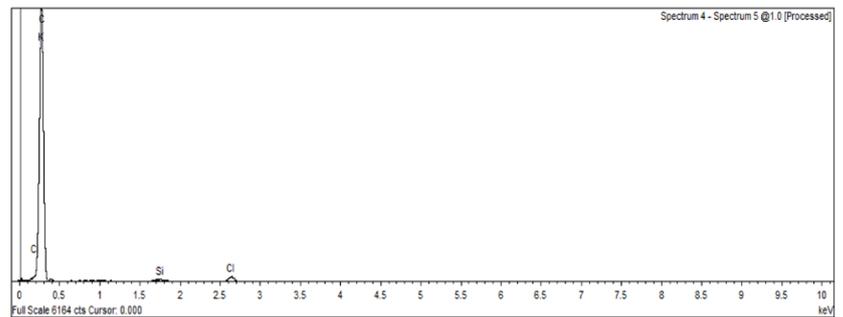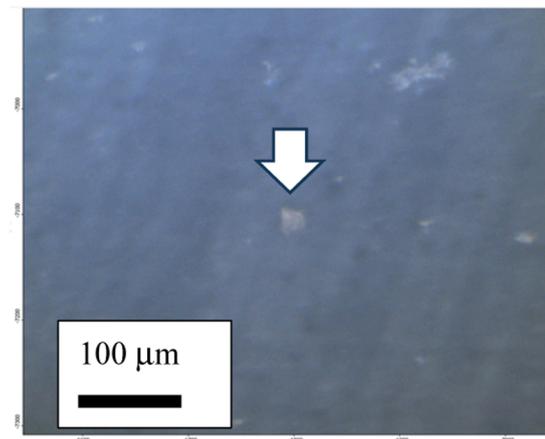
G
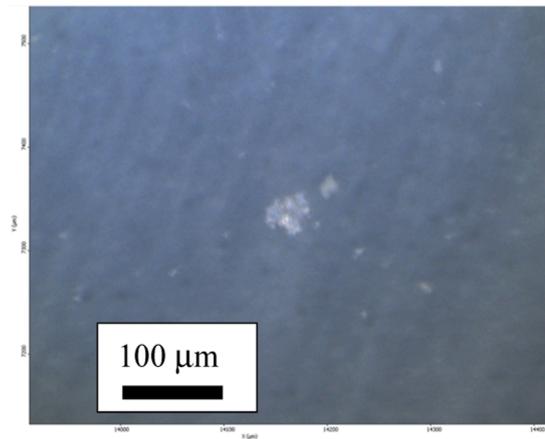
H Polyethylene (74% match)
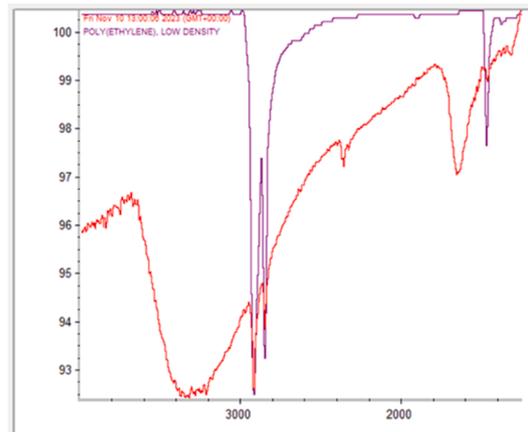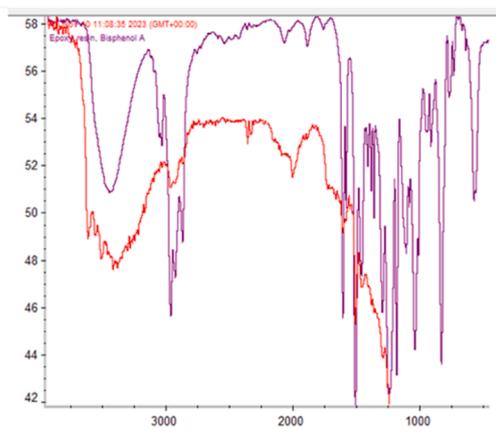

I

J

K

L Epoxy resin, bisphenol A (74% match)

Fig. 6. (*continued*).

are 10–20 times larger than previously considered possible for kidney filtration cut off, these are still 100–1000 times smaller than the MP particles detected in the urine samples herein. Rodent models expand the size range for potential kidney filtration into the MP size range as follows. 'Virgin' (un-weathered) 3 µm, 5 µm and 20 µm sized PS MP beads have been reported as taken up by mice following dietary exposure, or vein injection, from gut/vein to blood, liver, kidney, and urine (Deng et al., 2017; Wang et al., 2021; Sun et al., 2022; Xiong et al., 2023) (Table S2), highlighting differential gene expression of inflammation, oxidative stress, and apoptosis biomarkers in response to exposure

(Xiong et al., 2023). Differential gene expression of similar biomarker responses have similarly been reported in human kidney proximal tubular epithelial cells, HK-2, also exposed to 20 µm size PS MP beads, along with histopathological lesions and leaked protein levels in urine (Wang et al., 2021). An alternative route into urine for MPs, not involving the kidney, could be via the blood vessels serving the bladder (Fig. 6). The MP size and shape characteristics, along with the apparent conflict with kidney anatomy, are therefore key factors for further experiments in attempting to elucidate the human routes of MP uptake, their transport around the body, and consequent impact dynamics
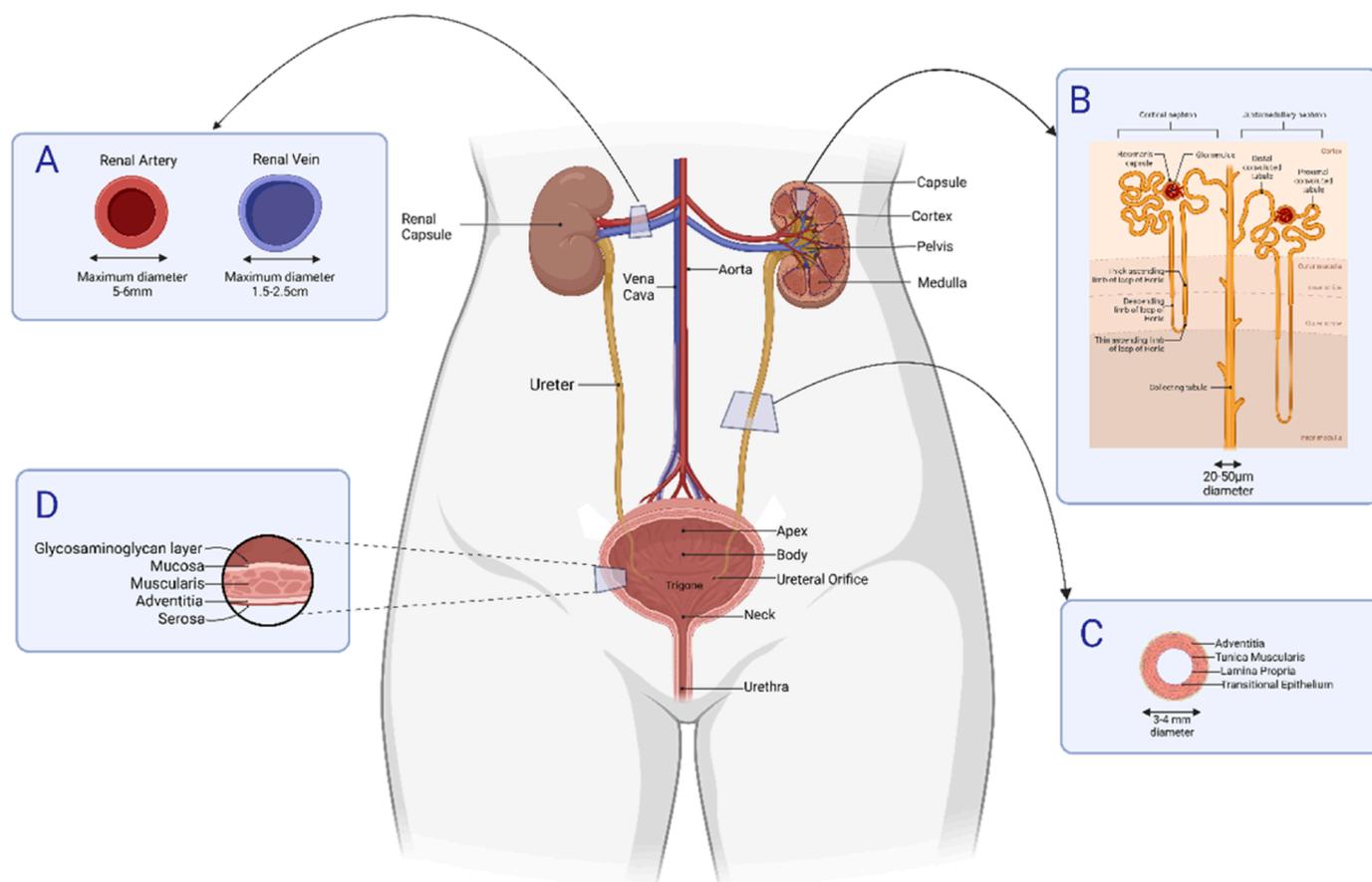
Fig. 7. Proposed MP transport to the bladder relative to the diameters of the internal tubules and associated blood vessels. A) renal arteries, branching from the aorta, and the renal veins drain into the inferior vena cava. The kidney is a fibrous capsule that can be divided into renal parenchyma consisting of two layers, a renal cortex and the renal medulla. The renal medulla consists of 10–14 renal pyramids (B), each separated renal columns where urine is made. Urine drains through the minor/major calyx and into the ureter (C). The ureter transports urine to the bladder. Its blood supply is segmental and includes the renal, common iliac and internal iliac arteries. Urine collects in the urinary bladder (D), which can hold 400–600 mL urine. During urination, the bladder contracts allowing urine to be expelled via the urethra. The bladder's main blood supply is the superior vesical branch of the internal iliac arteries with venous drainage into the internal iliac veins. (Created in BioRender.com).

thereafter.

This study also highlights important challenges in sampling for MPs from volunteer donors in settings that cannot be entirely choreographed or controlled such as clinics, homes, and hospitals. Previous work has highlighted that such settings can contain high levels of airborne at MPs 1924 $\pm$ 3105 MP m^{-2} day^{-1} in operating theatres (Field et al., 2022) and 1414 $\pm$ 1022 MP m^{-2} day^{-1} in indoor home environments (Jenner et al., 2021). No significant difference in MP levels between the air and water blanks were detected (p=0.247) although the main polymer types detected differed PE>PTFE>PS/PVC from air and PP>PE:PP from water-derived blanks. For comparison, a human lung tissue investigation reported a mean procedural blank MP contamination rate of 0.53 $\pm$ 1.07 MP per blank with four MPs identified: PE, PE/PP, PS, and a resin particle (Jenner et al., 2022b), like those identified in the current study blank samples (at ~1.7 MP per blank). A human vein tissue analysis reported a higher mean procedural blank MP contamination rate of 10.4 $\pm$ 9.21 MP per blank with four MP types PTFE>PP>PET> poly-fumaronitrile:styrene (FNS)(Rotchell et al., 2023). As highlighted in the literature (Noonan et al., 2023), procedural blanks are critical in determining between the MP types and levels within the urine samples and those that may represent airborne background contamination, which are unavoidable with a participant-led sampling procedure. The use of metal catheter-derived samples, along with clean room level of analysis using QA/QC approaches, would be the only way to reliably measure human urine samples, which would arguably not be practical for large numbers or population type monitoring approaches.

The observation of MPs in the human urine samples (from both healthy donors and endometriosis participants), displaying larger sizes than current paradigms would predict possible based on kidney filtration dynamics, led to the second batch of samples being analysed. The catheter approach and guided approach for healthy donors were adopted to remove, in the case of the catheter samples, or minimise/characterise in the case of the healthy donor provided urine plus parallel procedural blank samples, the source of intimate body-associated contaminating MPs (such as clothing materials). With these additional sampling procedure steps in place, MPs were still detected in human urine samples ruling out contamination as the source. All MP analyses of human derived samples, especially donor/participant-led, therefore require robust procedural blank methodologies and calculations to mitigate the unavoidable background contamination, with metal catheter sampling providing the most robust approach.

In addition to the MPs, several plastic monomers and additives were detected including the known endocrine disrupting chemical BPA. An EFSA Panel on Food Contact Materials, Enzymes and Processing Aids introduced a new tolerable daily intake value of 0.2 ng BPA/kg body weight as a result of evidence derived from animal and human observation studies highlighting immune system impacts (EFSA, 2023). Particles containing BPA were detected within 3/19 healthy donor and none of the endometriosis participant urine samples, with its presence consistent with other published studies from human and vertebrate urine samples (Table S2), thus adding to any calculation considerations in estimating a lifetime burden. Cellulose was the most abundant

non-MP particle type detected across urine samples in this study. Cellulose is used as an indicator that bacteria have entered the biofilm mode of growth highlighting potential urinary tract infections, and therefore not considered unusual as a common constituent in urine (Antypas et al., 2018).

In addition to the limitations of using µFTIR and SEM and spectra matches using libraries of virgin polymers discussed earlier, it is important to note that the µFTIR approach adopted herein used only one quarter of a filter (representing one quarter of the actual urine sample) for analysis. The values presented are the particles detected multiplied by four (to represent a whole filter). It is therefore possible that particles of other polymers were present but not detected. Also, calculations may contain rounding errors where the assumption has been made, potentially incorrectly, that particles of specific polymer types are evenly distributed upon a filter surface.

In conclusion, varying MP levels and types were detected and characterised in both healthy donor and endometriosis participant urine samples, and while the types and levels were not significantly different, the size ranges differed. The larger, irregular shaped MP particles identified in endometriosis participant urine samples (compared with the size range detected in the healthy donor samples) may lead inflammation-type responses, though this would require further cell toxicity and biomarkers of effects assays to establish. Endometriosis is a condition without clear causes, this study investigated whether the condition would correlate with urine MP levels, representing either a physical source of inflammation/stress or a possible pool of chemical leachate contaminants. MPs have been detected in urine samples. This raises important new questions with respect to their transport around the body and how they have traversed, or by-passed, the kidney glomerular filtration system with dimensions that are seemingly an order of magnitude too large to navigate such organs, as well as the potential biological impacts as a result of their presence.

CRediT authorship contribution statement

Kate Filart: Formal analysis. **Andrew Mead:** Resources. **Ben Blackburn:** Formal analysis. **Hannah Draper:** Writing – review & editing, Writing – original draft, Visualization, Supervision, Resources, Project administration, Methodology, Investigation, Funding acquisition, Formal analysis, Data curation, Conceptualization. **Chloe Austin:** Formal analysis. **Jane Allen:** Resources. **Jeanette Rotchell:** Writing – review & editing, Writing – original draft, Validation, Supervision, Project administration, Methodology, Investigation, Funding acquisition, Formal analysis, Data curation, Conceptualization. **Keith Cunningham:** Resources. **Ellie Beeby:** Formal analysis. **Timothy S. Dunstan:** Formal analysis. **Catriona R. Liddle:** Formal analysis. **Charlotte A. Atherall:** Formal analysis. **Barbara-ann Guinn:** Writing – review & editing, Writing – original draft, Visualization, Supervision, Resources, Project administration, Investigation, Funding acquisition, Formal analysis, Data curation, Conceptualization. **Emma Chapman:** Writing – review & editing, Writing – original draft, Visualization, Methodology, Investigation, Formal analysis, Data curation, Conceptualization.

Declaration of Competing Interest

The authors declare the following financial interests/personal relationships which may be considered as potential competing interests. Hannah Drape reports financial support was provided by British Society for Gynaecological Endoscopy grant to H.D and a Hull University Teaching Hospitals Clinical Fellowship to H.D. If there are other authors, they declare that they have no known competing financial interests or personal relationships that could have appeared to influence the work reported in this paper

Data Availability

Data will be made available on request.

Appendix A. Supporting information

Supplementary data associated with this article can be found in the online version at doi:10.1016/j.ecoenv.2024.116208.

References

Abramiuk, M., Grywalska, E., Malkowska, P., Sierawska, O., Hrynkiewicz, R., Niedzwiedzka-Rystwej, P., 2022. The role of the immune system in the development of endometriosis. Cells 11 (13), 2028. https://doi.org/10.3390/cells11132028.

Adhipandito, C.F., Cheung, S.H., Lin, Y.H., Wu, S.H., 2021. Atypical renal clearance of nanoparticles larger than the kidney filtration threshold. Int. J. Mol. Sci. 22, 11182. https://doi.org/10.3390/ijms222011182.

Amato-Lourenço, L.F., Carvalho-Oliveira, R., Júnior, G.R., dos Santos Galvão, L., Ando, R.A., Mauad, T., 2021. Presence of airborne microplastics in human lung tissue. J. Hazard. Mater. 416, 126124 https://doi.org/10.1016/j.jhazmat.2021.126124.

Antypas, H., Choong, F.X., Libberton, B., Brauner, A., Ricter-Dahlfors, A., 2018. Rapid diagnostic assay for detection of cellulose in urine as biomarker for biofilm-related urinary tract infections. Biofilm Micro 4, 26. https://doi.org/10.1038/s41522-018-0069-y.

Choi, W., Jung, H.R., Shehu, E., Rho, B.H., Lee, M.-Y., Kwon, K.Y., 2014. Small airway-centred granulomatosis by long-term exposure to polytetrafluoroethylene. Chest 145, 1397–1402. https://doi.org/10.1378/chest.13-1997.

Cowger, W., Booth, A.M., Hamilton, B.M., Thayson, C., Primpke, S., Munno, K., et al., 2020. Reporting guidelines to increase the reproducibility and comparability of research on microplastics. Appl. Spectrosc. 74, 1066–1077. https://doi.org/10.1177/0003702820930292.

Danopoulos, E., Twiddy, M., Rotchell, J.M., 2020b. Microplastic contamination of drinking water: a systematic review. PLOS ONE 15, e0236838. https://doi.org/10.1371/journal.pone.0236838.

Danopoulos E., Jenner L.C., Twiddy M., Rotchell J.M. (2020a). Microplastic contamination of seafood intended for human consumption: a systematic review and meta-analysis. Environ Health Perspect. 2020a;128 p.126002. doi:10.1289/ehp7171.

Danopoulos, E., Twiddy, M., West, R., Rotchell, J.M., 2021. A rapid review and meta-regression analyses of the toxicological impacts of microplastic exposure in human cells. J. Hazard. Mater. 427, 127861 https://doi.org/10.1016/j.jhazmat.2021.127861.

Deng, Y., Zhang, Y., Lemos, B., Ren, H., 2017. Tissue accumulation of microplastics in mice and biomarker responses suggest widespread health risks of exposure. Sci. Rep. 7, 46687 https://doi.org/10.1038/srep46687.

EFSA, European Food Safety Authority. Re-evaluation of the risks to public health related to the presence of bisphenol A (BPA) in foodstuffs. 2023, https://doi.org/10.2903/j.efsa.2023.6857.

Fenton, S.F., Ducatman, A., Boobis, A., DeWitt, J.C., Lau, C., Ng, C., Smith, J.S., Roberts, S.M., 2021. Per- and polyfluoroalkyl substance toxicity and human health review: current state of knowledge and strategies for informing future research. Environ. Toxicol. Chem. 40, 606–630.

Field, D.T., Green, J.L., Bennett, R., Jenner, L.C., Sadofsky, L.R., Chapman, E., Loubani, M., Rotchell, J.M., 2022. Microplastics in the surgical environment. Environ. Int. 170, 107630 https://doi.org/10.1016/j.envint.2022.107630.

Free, C.M., Jensen, O.P., Mason, S.A., Eriksen, M., Williamson, N.J., Boldgiv, B., 2014. High-levels of microplastic pollution in a large, remote, mountain lake. Mar. Pollut. Bull. 85, 156–163. https://doi.org/10.1016/j.marpolbul.2014.06.001.

GESAMP. Sources, fate and effects of microplastics in the marine environment: A global assessment. London UK: The Joint Group of Experts on Scientific Aspects of Marine Environmental Protection, Working Group 40. 2015.

Hammarstand, S., Jakobsson, K., Andersson, E., Xu, Y., Li, Y., Olovsson, M., Andersson, E.M., 2021. Perfluoroalkyl subtances (PFAS) in drinking water and risk for polycystic ovarian syndrome, uterine leiomyoma, and endometriosis: a Swedish

cohort study. Environ. Int. 157, 106819 https://doi.org/10.1016/j.envint.2021.106819.

Hartmann, N.B., Hüffer, T., Thompson, R.C., Hassellöv, M., Verschoor, A., Daugaard, A. E., et al., 2019. Are we speaking the same language? Recommendations for a definition and categorization framework for plastic debris. Environ. Sci. Technol. 53, 1039–1047. https://doi.org/10.1021/acs.est.8b05297.

Horton, A.A., Cross, R.K., Read, D.S., Jurgens, M.D., Ball, H.L., Svendsen, C., et al., 2021. Semi-automated analysis of microplastics in complex wastewater samples. Environ. Pollut. 268, 115841 https://doi.org/10.1016/j.envpol.2020.115841.

Horvatits, T., Tamminga, M., Liu, B., Sebode, M., Carambia, A., Fischer, L., et al., 2022. Microplastics detected in cirrhotic liver tissue. EBioMedicine 82, 104147. https://doi.org/10.1016/j.ebiom.2022.104147.

Ibrahim, Y.S., Tuan Anuar, S., Azmi, A.A., Wan Mohd Khalik, W.M.A., Lehata, S., Hamzah, S.R., et al., 2021. Detection of microplastics in human colectomy specimens. JGH Open 5, 116–121. https://doi.org/10.1002/jgh3.12457.

Jenner, L.C., Sadofsky, L.R., Danopoulos, E., Chapman, E., White, D., Jenkins, R.L., Rotchell, J.M., 2022a. Outdoor atmospheric microplastics within the Humber Region (United Kingdom): quantification and chemical characterisation of deposited particles present. Atmosphere 13, 265. https://doi.org/10.3390/atmos13020265.

Jenner, L.C., Sadofsky, L.R., Danopoulos, E., Rotchell, J.M., 2021. Household indoor microplastics within the Humber region (United Kingdom): Quantification and chemical characterisation of particles present. Atmos. Environ. 259, 118512 https://doi.org/10.1016/j.atmosenv.2021.118512.

Jenner, L.C., Rotchell, J.M., Bennett, R.T., Cowen, M., Tentzeris, V., Sadofsky, L.R., 2022b. Detection of microplastics in human lung tissue using µFTIR spectroscopy. Sci. Total Environ. 831, 154907 https://doi.org/10.1016/j.scitotenv.2022.154907.

Leslie, H.A., van Velzen, M.J.M., Brandsma, S.H., Vethaak, A.D., Garcia-Vallejo, J.J., Lamoree, M.H., 2022. Discovery and quantification of plastic particle pollution in human blood. Environ. Int. 163, 107199 https://doi.org/10.1016/j.envint.2022.107199.

Li, J., Green, C.G., Reynolds, A., Shi, H., Rotchell, J.M., 2018. Microplastics in mussels sampled from coastal waters and supermarkets in the United Kingdom. Environ. Pollut. 241 https://doi.org/10.1016/j.envpol.2018.05.038.

Molina, D.K., DiMaio, V.J., 2015. Normal organ weights in women: part II-the brain, lungs, liver, spleen, and kidneys. Am. J. Forensic Med. Pathol. 36, 182. https://doi.org/10.1097/PAF.0000000000000175.

Munno, K., Helm, P.A., Jackson, D.A., Rochman, C., Sims, A., 2018. Impacts of temperature and selected chemical digestion methods on microplastic particles. Environ. Toxicol. Chem. 37, 91–98. https://doi.org/10.1002/etc.3935.

Noonan, M.J., Grechi, N., Mills, C.L., de, A.M.M., Ferraz, M., 2023. Microplastics analytics: why we should not underestimate the importance of blank controls. Micro Nanoplast. 3, 17. https://doi.org/10.1186/s43591-023-00065-3.

Pagedar, N.A., Listinsky, C.M., Tucker, H.M., 2009. An unusual presentation of Teflon granuloma: case report and discussion. Ear Nose Throat J. 88, 746-7.

Pironti, C., Notarstefano, V., Ricciardi, M., Motta, O., Giorgini, E., Montano, L., 2023. First evidence of microplastics in human urine, a preliminary study of intake in the human body. Toxics 11, 40. https://doi.org/10.3390/toxics11010040.

Ragusa, A., Svelato, A., Santacroce, C., Catalano, P., Notarstefano, V., Carnevali, O., et al., 2021. Plasticenta: first evidence of microplastics in human placenta. Environ. Int 146, 106274. https://doi.org/10.1016/j.envint.2020.106274.

Ragusa, A., Notarstefano, V., Svelato, A., Belloni, A., Gioacchini, G., Blondeel, C., et al., 2022. Raman microspectroscopy detection and characterisation of microplastics in human breastmilk. Polymers 14, 2700. https://doi.org/10.3390/polym14132700.

Ramírez Carnero, A., Lestido-Cardama, A., Vazquez Loureiro, P., Barbosa-Pereira, L., Rodríguez Bernaldo de Quirós, A., Sendón, R., 2021. Presence of perfluoroalkyl and polyfluoroalkyl substances (PFAS) in food contact materials (FCM) and its migration to food. Foods 10, 1443. https://doi.org/10.3390/foods10071443.

Rotchell, J.M., Jenner, L.C., Chapman, E., Bennett, R., Bolanle, I.O., Loubani, M., Palmer, T., 2023. Detection of microplastics in human saphenous vein tissue using µFTIR: a pilot study. PLoS ONE 18, e0280594. https://doi.org/10.1371/journal.pone.0280594.

Ruggiero, A., Villa, C.H., Bander, E., McDevitt, M.R., et al., 2010. Paradoxical glomerular filtration of carbon nanotubes. Proc. Natl. Acad. Sci. U. S. A. 107, 12369–12374. https://doi.org/10.1073/pnas.0913667107.

Schwabl, P., Koeppel, S., Koenigshofer, P., Bucsics, T., Trauner, M., Reiberger, T., et al., 2019. Detection of various microplastics in human stool: a prospective case series. e457 Ann. Intern. Med. 171, 453. https://doi.org/10.7326/M19-0618.

Signorile, P.G., Viceconte, R., Baldi, A., 2022. New insights in pathogenesis of endometriosis. Front. Med. 9, 879015 https://doi.org/10.3389/fmed.2022.879015.

Sun, W., Jin, C., Bai, Y., Ma, R., Deng, Y., Gao, Y., et al., 2022. Blood uptake and urine excretion of nano- and micro-plastics after a single exposure. Sci. Total Environ. 848, 157639 https://doi.org/10.1016/j.scitotenv.2022.157639.

Vianello, A., Jensen, R.L., Liu, L., Vollertsen, J., 2019. Simulating human exposure to indoor airborne microplastics using a Breathing Thermal Manikin. Sci. Rep. 9, 8670. https://doi.org/10.1038/s41598-019-45054-w.

Wang, Y.-L., Lee, Y.-H., Hsu, Y.-H., Chiu, I.-J., Huang, C.C.-Y., Huang, C.-C., et al., 2021. The kidney-related effects of polystyrene microplastics on human kidney proximal tubular epithelial cells HK-2 and male C57BL/6 mice. Environ. Health Perspect. 129, 7612. https://doi.org/10.1289/EHP7612.

Wang, Z.M., Wagner, J., Ghosal, S., Bedi, G., Wall, S., 2017. SEM/EDS and optical microscopy analyses of microplastics in ocean trawl and fish guts. Sci. Total Environ. 603, 616–626.

Xiong, X., Gao, L., Chen, C., Zhu, K., Luo, P., Li, L., 2023. The microplastics exposure induce the kidney injury in mice revealed by RNA-seq. Ecotoxicol. Environ. Saf. 256, 114821 https://doi.org/10.1016/j.ecoenv.2023.2023.114821.

Yan, Z., Liu, Y., Zhang, T., Zhang, F., Ren, H., Zhang, Y., 2021. Analysis of microplastics in human feces reveals a correlation between fecal microplastics and inflammatory bowel disease status. Environ. Sci. Technol. 56, 414–421. https://doi.org/10.1021/acs.est.1c03924.

Yang, Y., Xie, E., Du, Z., Peng, Z., Han, Z., Li, L., et al., 2023. Detection of various microplastics in patients undergoing cardiac surgery. Environ. Sci. Technol. 57, 10911–10918.

Zhang, N., Li, Y.B., He, H.R., Zhang, J.F., Ma, G.S., 2021. You are what you eat: microplastics in the feces of young men living in Beijing. Sci. Total Environ. 767, 144345 https://doi.org/10.1016/j.scitotenv.2020.144345.

Zhao, Q., Zhu, L., Weng, J., Jin, Z., Cao, Y., Jiang, H., Zhang, Z., 2023. Detection and characterisation of microplastics in the human testis and semen. Sci. Total Environ. 877, 162713 https://doi.org/10.1016/j.scitotenv.2023.162713.